ACADEMIA ROMÂNĂ
Revue Roumaine de Chimie
https://www.icf.ro/rrch/

Rev. Roum. Chim.,
2024, *69*(3–4), 139–148
DOI: 10.33224/rrch.2024.69.3-4.04

EXPERIMENTAL AND THEORETICAL STUDIES OF AMINOTHIOPHENE DERIVATIVES INHIBITORS ON CARBON STEEL CORROSION IN PERCHLORIC ACID MEDIUM

Yazid DATOUSSAID,[a,b*] Hadjer MISSOUM,[b] Tarik ATTAR,[a,c] Boulanouar MESSAOUDI,[a,c] Abbes BENCHADLI,[c], Esma CHOUKCHOU-BRAHAM,[c] Noureddine Choukchou-Braham[b] and Chewki ZIANI-CHERIF [b]

[a]Higher School of Applied Sciences of Tlemcen (ESSAT), 13000 Tlemcen, Algeria
[b]Laboratory of Catalysis and Synthesis in Organic Chemistry, Faculty of Sciences, University of Abou Bekr Belkaid BP 119,13000 Tlemcen, Algeria
[c] Laboratory of ToxicoMed, University of Abou Bekr Belkaïd, B.P.119, Tlemcen, 13000, Algeria

Received June 1, 2023

The effect of two aminothiophene derivatives, namely (2-amino-4-phenylthiophene-3-carbonitrile) APTC and (2-amino-4-p-tolylthiophene-3-carbonitrile) ATTC, as carbon steel corrosion inhibitors in a perchloric acid medium was investigated. The study was performed by weight loss method, quantum chemical calculations (DFT) and Scanning electron microscope (SEM).

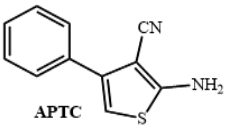

APTC
2-amino-4-phenylthiophene-3-carbonitrile

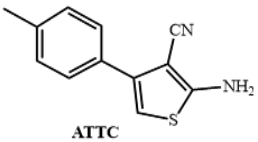

ATTC
2-amino-4-*p*-tolylthiophene-3-carbonitrile

The impact of the two aminothiophene derivatives as inhibitors was positively correlated with concentration, temperature, and exposure time. The value of the active energy of the inhibition corrosion reaction of carbon steel is greater than that obtained for the blank solution. All experimental data were consistent with the Langmuir adsorption isotherm, and the value and sign of the adsorption free energy obtained indicated that the inhibitor molecules were spontaneously adsorbed on the carbon surface by a mixed adsorption mechanism. The SEM surface analysis showed the formation of a protective organic film on the steel surface. The DFT supported the experimental results and showed that the inhibition effect is structure-dependent.

INTRODUCTION

Corrosion is a major global problem that strongly affects the natural and industrial environment.[1] According to the World Corrosion Organization (WTO), the cost of corrosion represents today 3 to 4% of the GDP of industrialized countries. In industry, direct and long-standing contact of metals with aggressive media represents one of the main causes of corrosion. Notwithstanding, high strength carbon steel remains a primary choice for most equipment and installation infrastructures, since it is known to suffer the least when exposed to aggressive media.[2,3] To remedy to the problem, retreatment is often used to strengthen the steel layer and improve its resistance to corrosion. Several techniques have been developed and lead to modifications of the surface of the material. Traditionally, in industry, organic inhibitors have established themselves as an effective solution. They are available at low cost and are more respectful to the environmental standards.[4] The search for potential organic corrosion inhibitors was for a long time based on trial and error; it found that the most effective and efficient

* Corresponding author: datouyazid@gmail.com

inhibitors are the organic compounds that include π bonds and heteroatoms (P, S, N, and O) in their main frame, likely to form chemical bonds with metals and their alloys, as well as carbon rings capable of interacting with the surface of the substrate via the π electrons of the double bonds.[5] Compounds containing sulfur heteroatoms can be considered safe corrosion inhibitors, because they are environmentally friendly, non-toxic, biodegradable and relatively inexpensive.[6] Among the compounds that contain sulfur heteroatom, Thiophene and its derivatives are the much studied and cited in the literature. They possesses a wide range of activities,[7–12] which mainly depend on the nature of the substituents.

The selection of thiophene derivatives with different substituents as corrosion inhibitors is based on the presence of an electron-rich aromatic system along with sulfur atoms in the conjugated system, which facilitates eventual electrophilic attack. Quantum chemical calculation has become a very useful tool supportive of mechanism rationalization and explanation. In the present context, density functional theory (DFT) was run to estimate and theoretically correlate the reactivity parameters of the inhibitor.

As a continuation to our efforts toward potent anti-corrosive discovery, we wish to report on the synthesis of (2-amino-4-phenylthiophene-3-carbonitrile) APTC and (2-amino-4-p-tolylthiophene-3-carbonitrile) ATTC, as well as their anti-corrosive activity.

MATERIALS AND METHODS

The preparation of thiophene derivatives

We developed since a while interest in the development and functionalization of heterocyclic compounds.[13] As a part of our research, we introduced the popular Vilmeier-Haack reaction in the synthesis of new heterocyclic systems combining easiness and efficiency. Hence, through a modification of the Gewald reaction,[14] we obtained derivatives of 2-amino-3-cyanothiophene, which contain two (2) reactive sites (Fig. 1)

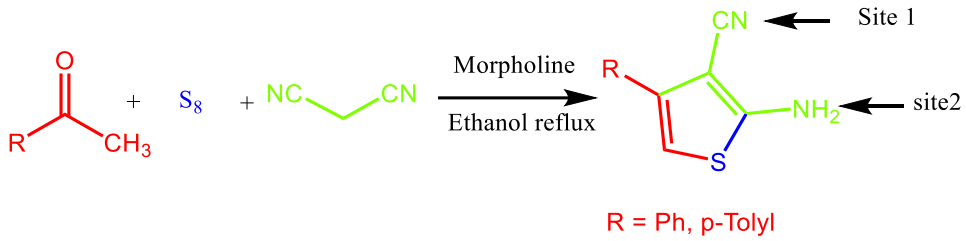

Fig. 1 – Synthesis of APTC and ATTC by a modification of the Gewald reaction.

In the present work, thiophene derivatives (see Fig. 2), namely, (2-amino-4-phenylthiophene-3-carbonitrile) APTC and (2-amino-4-p-tolylthiophene-3-carbonitrile) ATTC (C), have been chosen for anticorrosive activity studies.

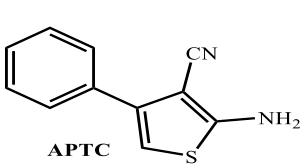

APTC
2-amino-4-phenylthiophene-3-carbonitrile

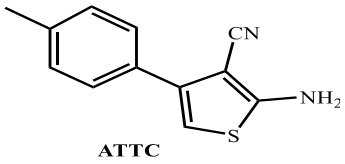

ATTC
2-amino-4-*p*-tolylthiophene-3-carbonitrile

Fig. 2 – Chemical structures of APTC and ATTC.

Material Preparation

The carbon steel's composition used as a working electrode was (%wt): C: 0.37%, Mn: 0.68%, Cu: 0.16%, Cr: 0.077%, Ni: 0.059%, Si: 0.023%, S: 0.016%, Ti: 0.011%, Co: 0.009% and the remaining was Fe. The solution of 1M perchloric acid was prepared by diluting HClO4 (99%, Sigma Aldrich, Germany) with double distilled water.

Gravimetric method

Weight loss methods give more realistic results in terms of uniform corrosion than electrochemical methods because the experimental conditions

correspond to real conditions. The same procedures described in our previous work by Attar[15-17] were used for the weight loss measurements. All measurements were taken in triplicate and the mean value of the weight loss was given and recorded.

The corrosion rate CR and the effectiveness of the inhibitor were calculated using the following equation.[18]

$$CR = \frac{\Delta w}{S} t \quad (1)$$

where Δw denotes the weight loss (mg), S represents the sample area (cm^2) and t symbolizes the immersion time (h).

The corrosion inhibition efficiency (IE %) and surface coverage (θ) were calculated from the values of CR[19]

$$IE = \frac{100x(CR - CR_{Inh})}{CR} \quad (2)$$

$$\theta = \frac{IE}{100} \quad (3)$$

where CR and CR_{inh} denote the corrosion rates obtained in the absence and presence of the inhibitor, respectively.

RESULTS AND DISCUSSION

Effect of concentration and immersion time on corrosion rates and inhibition Efficiency

Exposure time and concentration are important parameters that determine the inhibitory effect on metallic surfaces.[20] The effects of exposure time on the corrosion behaviour of carbon steel in 1M $HClO_4$ solution without then with different concentrations of the two inhibitors were investigated at a temperature of 303 K. To such an end, the corrosion rate and inhibition effect of APTC and ATTC inhibitors were determined after 1, 2, 4, 6, and 24 hours of exposure (Table 1).

Table 1

Corrosion rate, inhibition efficiency and surface coverage of carbon steel in 1 M $HClO_4$ in the absence and presence of the two inhibitors at different concentrations at 303 K

		Acetophanone APTC			Methyl acetophenone ATTC		
C (mol/L)	Time (hrs)	CR (mg/hcm^2)	EI (%)	θ	CR (mg/hcm^2)	EI (%)	θ
–	1	2.001	–	–	–	–	–
	2	3.598	–	–	–	–	–
	4	4.392	–	–	–	–	–
	6	5.511	–	–	–	–	–
	24	6.491	–	–	–	–	–
5.0×10^{-6}	1	1.239	38.08	0.38	0.929	53.57	0.53
	2	1.998	44.45	0.44	1.190	66.92	0.66
	4	2.751	37.36	0.37	2.141	51.25	0.51
	6	3.605	34.58	0.34	2.812	48.97	0.48
	24	4.508	30.55	0.30	3.541	45.44	0.45
1.0×10^{-5}	1	0.944	52.82	0.52	0.901	54.97	0.54
	2	1.251	65.23	0.65	0.928	74.21	0.74
	4	2.092	52.36	0.52	1.801	58.99	0.58
	6	2.859	48.12	0.48	2.620	52.45	0.52
	24	3.641	43.90	0.43	3.321	48.83	0.48
5.0×10^{-5}	1	0.669	66.56	0.66	0.575	71.26	0.71
	2	0.796	77.88	0.77	0.579	83.91	0.83
	4	1.461	66.73	0.66	1.071	75.61	0.75
	6	2.318	57.93	0.57	1.989	63.90	0.63
	24	2.989	53.95	0.53	2.723	58.04	0.58
7.5×10^{-5}	1	0.573	71.36	0.71	0.491	75.46	0.75
	2	0.769	78.62	0.78	0.499	86.13	0.86
	4	1.311	70.15	0.70	1.031	76.52	0.76
	6	1.992	63.85	0.63	1.747	68.29	0.68
	24	2.571	60.39	0.60	2.372	63.45	0.63
7.5×10^{-4}	1	0.497	75.16	0.75	0.363	81.85	0.81
	2	0.331	90.83	0.90	0.151	95.80	0.95
	4	0.719	83.62	0.83	0.608	86.15	0.86
	6	1.507	72.65	0.72	1.221	77.84	0.77
	24	2.011	69.01	0.69	1.679	74.13	0.74

Gravimetric measurements show that the corrosion rate decreases in the presence of APTC and ATTC. Their inhibitory effect is better expressed by the inhibition efficiency, which increases with inhibitor concentration, reaching almost 90 and 96 % at 7.5×10^{-4} mol/L for APTC and ATTC, respectively. Two hours is the optimal exposure time for the inhibitory effect of APTC and ATTC. After this time, the inhibitory effect decreased, either due to decomposition, desorption and/or instability of these inhibitors. Finally, we found that ATTC has a slight advantage over APTC.

Effect of temperature

Temperature is another important parameter that can alter the interactions between the carbon steel and the perchloric acid in the absence and presence of the inhibitors. The effect of temperature on the corrosion of carbon steel in 1 mol·L^{-1} $HClO_4$ was determined by measuring the weight loss in the range of 293 to 323 K after 2 hours of immersion using different concentrations of the two inhibitors (APTC and ATTC), going from 5.0×10^{-6} to 7.5×10^{-4} mol/L (Fig. 3).

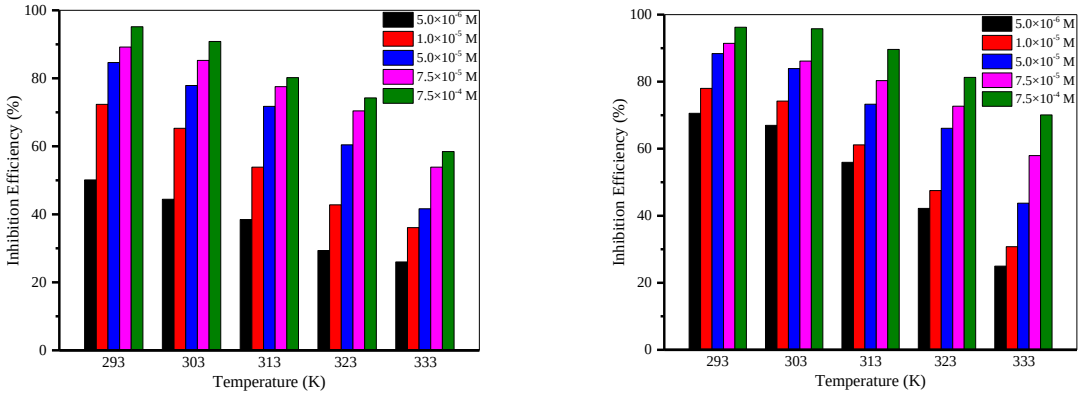

Fig. 3 – Variation of the inhibitory effect (IE %) with solution temperature (293–333 K) at different concentrations of APTC (left) and ATTC (right).

The corrosion rates of carbon steel in free and inhibited acidic media increased with increasing temperature, but to different degrees. This behaviour reflects a decrease in the inhibitory effect (I.E %) of the inhibitors with temperature. The decreasing tendency of I.E. can be attributed to a temperature-dependent adsorption/desorption process that shifts the equilibrium towards the desorption process, leading to a decrease in surface coverage.[21,22] It is also noted that this decrease is less pronounced in the ATTC compound, indicating a possible influence of the methyl substituent.[23,24] This observation suggests that the protective mechanism is due to the physical adsorption of the organic compound on the surface of the carbon steel.

Thermodynamic activation functions of the corrosion process

The kinetics of inhibited aggregation can be understood in terms of thermodynamic and activation parameters. The Arrhenius and transition state equations have been successfully used to show the influence of temperature on the inhibitory effect of the studied inhibitor. In the absence and presence of a mixture, the activation energy, also known as E_{act}, the enthalpy, or ΔH_{act}, and the entropy, also known as ΔS_{act}, can be used to study the kinetics of inhibitory activity. It is represented by the following equations:[25]

$$CR = A \times \exp\left(-\frac{E_{act}}{RT}\right) \quad (4)$$

$$\mathbf{Ln}\left(\mathbf{CR}/\mathbf{T}\right) = \left[\mathrm{Ln}\left(\mathbf{R}/\mathbf{Nh} + \mathbf{\Delta S_{act}}/\mathbf{R}\right)\right] - \mathbf{\Delta H_{act}}/\mathbf{RT} \quad (5)$$

where CR is the corrosion rate of carbon steel, A is the Arrhenius pre-exponential factor, R is the gas constant, and T is the temperature, N is Avogadro's number and h is Plank's constant.

As depicted in Fig. 4(a, b), Equation (4) can be shown as the natural logarithm of corrosion rate (ln (CR)) against the reciprocal of absolute temperature (1/T). Equation (5) can be represented in Fig. 5(c, d) as the natural logarithm of corrosion rate (ln (CR/T)) against the reciprocal of absolute temperature (1/T). Using the slopes of the Arrhenius and transition state equations, activation energy values (E_{act}) and activation enthalpy (ΔH_{act}) can be calculated respectively.

The values of entropy change were obtained from the intercepts of the plots ln(CR/T) *versus* 1/T of Fig. 5.

The change in the free energy of activation (ΔG_{act}) of the corrosion process can be determined at any temperature by using the equation.[26]

$$\Delta G_{act} = \Delta H_{act} - T\,\Delta S_{act} \quad (6)$$

All these parameters (E_{act}, ΔH_{act}, ΔS_{act} and ΔG_{act} at 303K) are collected in Table 2.

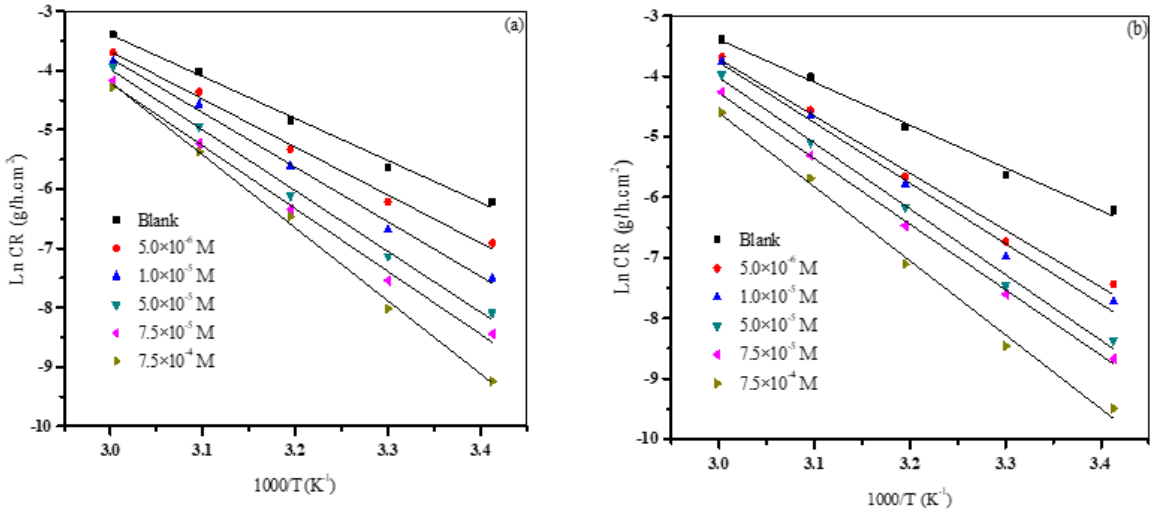

Fig. 4 – Arrhenius plot for the dissolution of Carbon Steel in 1 M $HClO_4$ without and with different concentrations of APTC (a) and ATTC (b) at various temperatures.

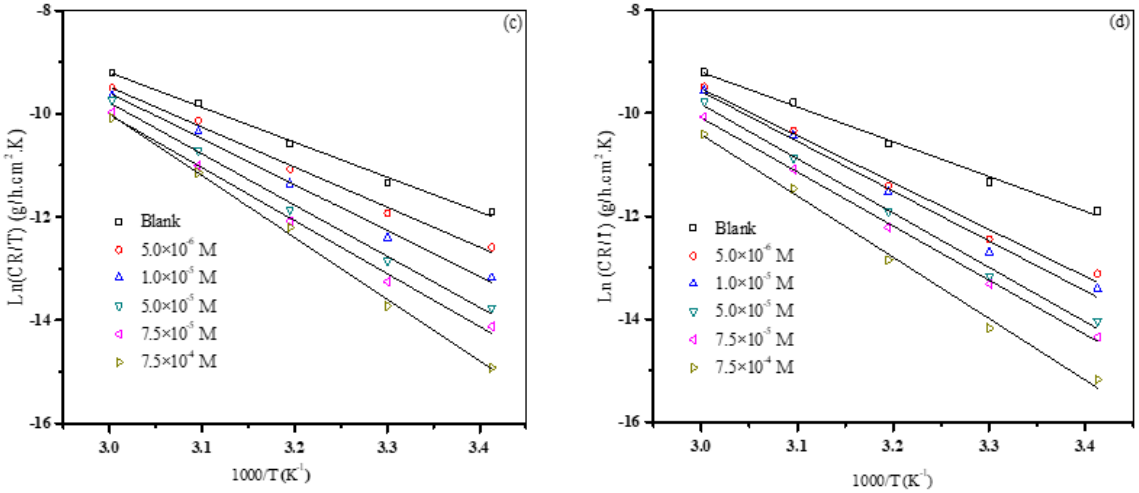

Fig. 5. – Curves ln (W/T) *versus* 1/T for carbon steel dissolution in absence and presence of different concentrations of APTC (c) and ATTC (d) in 1 M $HClO_4$ solution .

In the presence of both inhibitors, the activation energy was greater than in the uninhibited solution. The higher value of the free activation energy in the inhibited system indicates that the inhibitors are more effective at lower temperatures.[26] The E_{act} in the inhibited acid ranged from 67.16 to 102.19 kJ mol^{-1}, indicating that the strong inhibitory effect of the inhibitors arises from an increase in the energy barrier to the corrosion process. This in return emphasises the electrostatic nature of the inhibitor (physisorption).[27] A positive value of the activation enthalpy (ΔH_{act}) means that the dissolution of carbon steel in acidic solution is endothermic. The negative sign of the change in entropy in the absence and presence of the inhibitors indicates that the activation complex is the decisive step, which appears to be an association step and not a dissociation phase[24]. The free activation energy shows that the corrosion reaction of carbon steel is not spontaneous and increases with increasing the inhibitor concentration. The higher values (ΔG_{act}) of the process in the presence of the two inhibitors compared to those in their absence are due to their physisorption, while the opposite is true for chemisorption.

Table 2

The values of activation parameters for carbon steel in 1M $HClO_4$ in the absence and presence of APTC and ATTC at divesrse concentrations

	C (mol/L)	E_{act} (KJ/mol)	ΔH_{act} (KJ/mol)	ΔS_{act} (J/mol K)	$\Delta G_{act\ (at\ 313\ K)}$ (KJ/mol)
Blank	1	58.79	56.20	–105.43	89.19
APTC	5.0×10^{-6}	67.16	64.56	–82.66	90.43
	1.0×10^{-5}	76.49	73.90	–55.62	91.30
	5.0×10^{-5}	85.11	82.52	–31.32	92.32
	7.5×10^{-5}	87.97	85.38	–24.70	93.11
	7.5×10^{-4}	102.19	99.60	–18.09	105.26
ATTC	5.0×10^{-6}	78.42	75.82	–49.23	91.22
	1.0×10^{-5}	83.09	80.49	–35.67	91.65
	5.0×10^{-5}	90.37	87.77	–15.91	92.74
	7.5×10^{-5}	90.09	87.50	–18.90	93.41
	7.5×10^{-4}	101.74	99.15	–13.35	103.32

Adsorption isotherm and inhibition mechanism

The adsorption isotherm explains the relationship between the amount of adsorbate fixed on an adsorbent, and the concentration of adsorbate in solution when equilibrium is reached at constant temperature. It was found that the Langmuir adsorption isotherm best describes adsorption. According to the Langmuir adsorption isotherm, a carbon steel surface has a fixed number of adsorption sites, each of which can hold only a single adsorbed molecule. Surface coverage results are in full agreement with the weight loss method in the presence of inhibitors. The Langmuir adsorption isotherm can be represented as follows:

$$C/\theta = 1/K_{ads} + C \quad (7)$$

where C is the inhibitor concentration, θ is the degree of coverage on the metal surface and K_{ads} is the equilibrium constant for adsorption desorption process, calculated by the reciprocal of the intercept of isotherm line at different temperatures.

The free energy of adsorption (ΔG_{ads}) on carbon steel surface can be evaluated with the following equation (8)[16]

$$\Delta G_{ads} = -RT\ \ln(55.5K_{ads}) \quad (8)$$

where R is the gas constant (J mol^{-1} K^{-1}) and T is the absolute temperature (K). The constant value of 55.5 is the concentration of water in solution (mol L^{-1}).

Table 3

Thermodynamic parameters for the adsorption of inhibitors in 1M $HClO_4$ solution on carbon steel at different temperatures

	T (K)	K_{ads} (m^3/mol)	ΔH_{ads} (kJ/mol)	ΔS_{ads} (J/mol K)	ΔG_{ads} (kJ/mol)
APTC	293	194.21	–23.61	54.02	–39.44
	303	156.11		54.88	–40.24
	313	162.05		57.66	–41.66
	323	92.55		55.35	–41.49
	333	57.73		53.63	–41.47
ATTC	293	297.31	–37.34	10.71	–40.48
	303	182.51		10.85	–40.63
	313	126.93		11.78	–41.03
	323	97.69		13.31	–41.64
	333	40.09		9.36	–40.46

The thermodynamic parameters for the adsorption of inhibitors can provide valuable information on the mechanism of corrosion inhibition. The decreasing K_{ads} values with increasing temperature indicate that the adsorption improves at low temperatures. This decrease in the adsorption equilibrium constant indicates that the adsorbed inhibitor tends to desorb from the metal surface again at a higher temperature.[20] The negative values of ΔH_{ads} (–23.61 and –37.34 kJ mol^{-1}) for both inhibitors indicate that adsorption on the metal surface is exothermic. The variation of the free energy of adsorption between –39.44 and –41.66 kJ mol^{-1} suggests that the adsorption of the two inhibitors on the metal surface is a mixture of both chemical and physical sorption. Moreover, the negative ΔG_{ads} values indicate that the adsorption of the inhibitors on the metal surface is spontaneous. In general, adsorption is an exothermic process that is always accompanied by a decrease in entropy. This is explained by an increase in disorder during the conversion of the reactants into the activated complexes. The result shows that the two compounds used act as good inhibitors for the corrosion of carbon steel in perchloric acid.

Scanning Electron Microscopy (SEM)

Figure 6 shows SEM images of the uninhibited carbon steel before and after immersion in 1M $HClO_4$ and the inhibited carbon steel with the best corrosion performance of the two inhibitors at 7.5×10^{-4} M. It can be seen from the images that the metal surface of the samples immersed in perchloric acid has a rough and more clearly corroded surface due to the acid attack. However, the microscopic image of the surface inhibited with APTC or ATTC shows a smoother surface due to the formation of a protective film that prevents the corrosion attack, confirming inhibition efficiency. A similar observation has already been reported in the literature.[28]

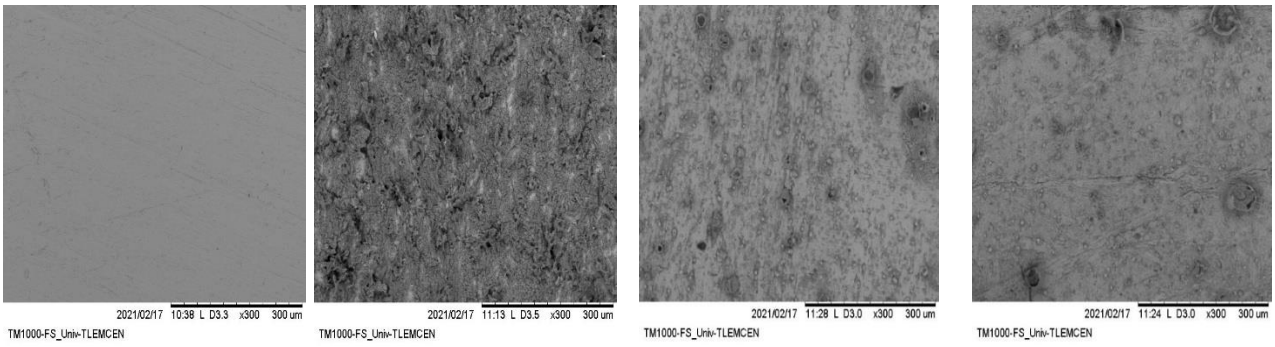

(a) (b) (c) (d)

Fig. 6 – SEM images of carbon steel samples: a) before immersion; b) after immersion in 1M $HClO_4$; c) after immersion with 7.5×10^{-4}M of APTC; d) after immersion with 7.5×10^{-4}M of ATTC.

Quantum chemical calculation

The electronic properties of the inhibitors were studied using density functional theory (DFT)-B3LYP/6-31G*. Optimized structure, HOMO and LUMO were studied for three molecules and shown in Fig. 7. The studied energy parameters of the frontier molecular electrons, global hardness, gap energy, backdonation and number of transferred electrons are shown in Table 4.

The values of the highest molecular orbitals (HOMO) of the two molecules studied increase in the following order: ATTC > APTC, which means that the first inhibitor has the highest inhibitory effect and the best inhibitory power, which agrees well with the experimental measurements. There is also an increasing trend in E_{LUMO} (ATTC > APTC), which shows that the electron acceptor's ability becomes weaker. In the literature, it is assumed that the lower the values of the gap energy levels, the higher the inhibition efficiency are.[29] This study corroborates just that, as the energy gap of ATTC is smaller than that of APTC. In addition, the molecule with the lowest chemical hardness should have the greatest inhibitory effect. The results show that the ΔN values correlate strongly with the experimental inhibition effects. This is in good agreement with the experimental observations (ΔN must be less than 3.6 eV).[22, 24] The $\Delta E_{back\text{-}donation}$ values for the two inhibitors are negative, indicating that back-donation is desirable for these materials and leads to strong binding.[30]

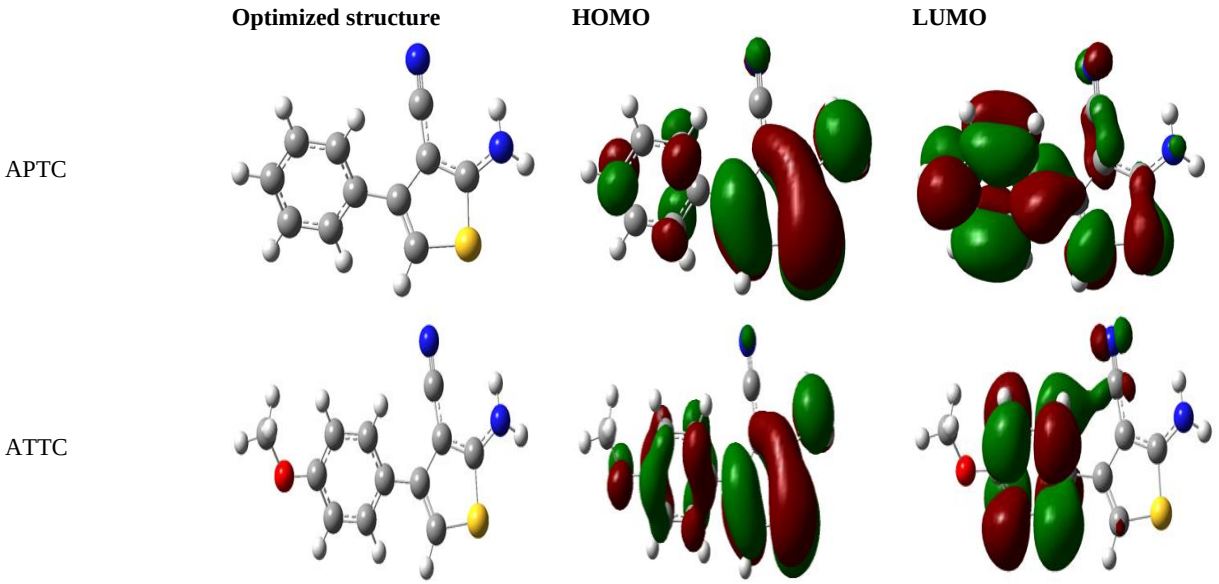

Fig. 7 – The frontier molecular orbital density distributions and the optimized structure of APTC and ATTC.

Table 4

HOMO and LUMO energies, global reactivity indices η, ω, ΔE_{gap}, ΔN and $\Delta E_{back\text{-}donation}$ for the A**PTC** and **ATTC** studied compoundsB3LYP/6-31G* level of theory.

Substrate	HOMO (eV)	LUMO (eV)	ΔE_{gap} (eV)	η (eV)	ΔN (eV)	$\Delta E_{back\text{-}donation}$
APTC	–5.74	–0.88	4.86	2.43	0.75	–0.60
ATTC	–5.50	–0.73	4.77	2.38	0.81	–0.59

Mechanism of inhibition

The inhibitory effect of the aminothiophene derivatives solutions on carbon steel corrosion in perchloric acid can be attributed to the adsorption of these compounds at the interface between metal and solution.

As mentioned above, the inhibition efficiency increased with the rise of ATTC and APTC concentration. This can be attributed to the increase in carbon steel surface covered by the adsorbed molecules. Based on the aforementioned experimental and theoretical analyses, as both ATTC and APTC inhibitors contain nitrogen and sulfur atoms, they can be protonated easily. During the inhibition process, the inhibitors are protonated in solution and become positively charged, as well as the metal surface in the acid medium (Chimisorption).

Perchlorate ions are specifically adsorbed on the metal and create an excess of negative charge on its surface. They promote the adsorption of protonated ATTC and APTC on the surface by electrostatic attraction and therefore reduce the dissolution of iron (Physical adsorption).

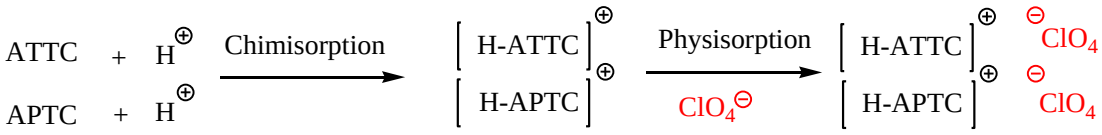

The electron-rich properties of the benzene ring in ATTC and APTC may also contribute to the adsorption of the inhibitor molecules through the electrostatic attraction with the vacant orbital d of the metal (Retrodonation). The slight advantage in terms of inhibition for ATTC compared to APTC is due to the presence of the inductive donor effect of the methyl group in the para position, which leads to a higher electronic density of the phenyl group within the p-tolyl, therefore an electrostatic force slightly greater than that of the phenyl alone of the APTC compound. In summary, the adsorption of APTC and ATTC on the surface of carbon steel is complete and includes both physisorption and chemisorption.

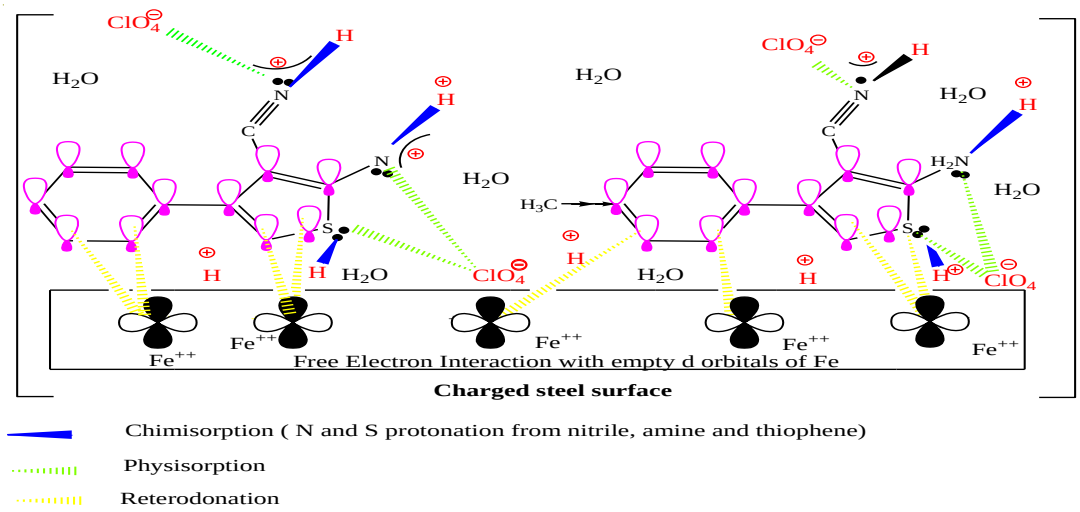

Fig. 8 – The suggested mechanism of ATTC and APTC for carbon steel in perchloric acid solution.

CONCLUSION

The two compounds used in this study were found to be effective corrosion inhibitors for carbon steel surfaces in 1.0 M perchloric acid. The effectiveness depends on the temperature and concentration. The inhibition efficiency increases with increasing concentration of the inhibitor, but decreases with increasing temperature. The adsorption isotherms of ATTC and APTC on the steel surface correlate with the Langmuir adsorption isotherm. The negative sign of the free energy indicates a spontaneous adsorption process. The values of activation energy and change in adsorption free enthalpy indicate the presence of both physisorption and chemisorption. Before and after the corrosion process, the scanning electron microscope proved to be an effective tool to confirm the weight loss results. The quantum chemical calculations are in good agreement with the experimental results.

REFERENCES

1. B. Valdez, M. Schorr, R. Zlatev, M. Carrillo, M. Stoytcheva, L. Alvarez, A. Eliezer and N. Rosas, "Environmental and Industrial Corrosion-Practical and Theoretical Aspects", 2012.
2. D. Dwivedi, K. Lepková and T. Becker, *RSC advances*, **2017**, *7*, 4580–4610.
3. T. Attar, B. Messaoudi, A. Benchadli, I. Seghiouer, M. A. Zenasni, S. Bousalem and E. Choukchou-braham. *Rev. Roum. Chim*., **2021**, *66*, 761–770.
4. M. A. Malik, M. A. Hashim, F. Nabi, S. A. Al-Thabaiti and Z. Khan, *Int. J. Electrochem. Sci.*, **2011**, *6*, 1927–1948.
5. H. Assad and A. Kumar, *J. Molec. Liquids.*, **2021**, *344*, 117755–117762.
6. B. A. Al Jahdaly, Y. R. Maghraby, A. H. Ibrahim, K. R. Shouier, M. M. Taher and R. M. El-Shabasy, *Materials Today Sustainability*, **2022**, 100242–100250.
7. L. Berrade, B. Aisa, M. J. Ramirez, S. Galiano, S. Guccione, L. R. Moltzau, F. O. Levy, F. Nicoletti, G. Battaglia and G. Molinaro, *J. Medicinal Chem.*, **2011**, *54*, 3086–3090.
8. S. M. Sondhi, S. Jain, M. Dinodia and A. Kumar, *Medicinal Chem.*, **2008**, *4*, 146–154.
9. L. N. de Araújo Neto, M. d. C. A. de Lima, J. F. de Oliveira, E. R. de Souza, M. D. S. Buonafina, M. N. V. Anjos, F. A. Brayner, L. C. Alves, R. P. Neves and F. J. B. Mendonça-Junior, *Chem.-Biol. Interactions*, **2017**, *272*, 172–181.
10. M. Rani and Y. Mohamad, *J.Saudi Chem. Soc.*, **2014**, *18*, 411–417.
11. M. Albratty, K. A. El-Sharkawy and H. A. Alhazmi, *Acta Pharma.*, **2019**, *69*, 261–276.
12. M. K. Parai, G. Panda, V. Chaturvedi, Y. Manju and S. Sinha, *Bioorg. & Medicinal Chem. Lett.*, **2008**, *18*, 289–292.
13. a-Y. Datoussaid, G. Kirsch, A. A. Othman and I. Abdillahi, *South African J. Chem.*, **2012**, *65*, 223–227; b-D. Yazid, A.-D. Tewfik, M. Nawel, L. Brahmi, K. Zahira, H. Rachida and C.-B. Noureddine, *Lett. in Org. Chem.*, **2022**, *19*, 347–352.
14. A. B. Abdelwahab, A. G. Hanna and G. Kirsch, *Synthesis*, **2017**, *49*, 2971–2979.
15. A. Benchadli, T. Mellal, T. Attar, B. Dali Youcef and E. Choukchou-Braham, *Rev. Mex. Fís.*, **2022**, *68*, 1–11.
16. A. Benchadli, T. Attar and E. Choukchou-Braham, *Phys. Chem. Res.*, **2019**, *7*, 837–848.
17. T. Attar, A. Benchadli, B. Messaoudi and E. Choukchou-Braham. *Chem. Technol*., **2022**, *16*, 440–447.
18. I. Danaee, S. Ramesh Kumer, M. Rashvand Aveic and M. Vijayan, *J. Mater. Res.*, **2020**, *23*, 1–16.
19. A. Benchadli, T. Attar and E. Choukchou-Braham, *JARST*, **2018**, *5*, 834–844.
20. T. Attar, A. Benchadli, B. Messaoudi, N. Benhadria and E. Choukchou-Braham, *Bull. Chem. React. Eng. Catal.*, **2020**, *15*, 454–464.
21. M. P. Chakravarthy and K. N. Mohana, *Int. Sch. Res.*, **2014**, 1–13.
22. A. Benchadli. T. Attar, B. Messaoudi and E. Choukchou Braham, *Hungarian J. Ind. Chem.* **2021**, *49*, 59–69.

23. M. E. Mashuga, L. Olasunkanmi, A. S. Adekunle, S. Yesudass, M. M. Kabanda and E. E Ebenso, *Materials*., **2015,** *8*, 3607–3632.
24. T. Attar, F. Nouali, Z. Kibou, A. Benchadli, B. Messaoudi, E. Choukchou-Braham and N. Choukchou-Braham, *J. Chem. Sci.*, **2021**, *133*, 1–10.
25. A. A. Khadom, A. N. Abd and N. A. Ahmed, *S. Afr. J. Chem. Eng.*, **2018**, *25*, 13–21.
26. T. Attar, A. Benchadli, B. Messaoudi and E. Choukchou-Braham, *Fr. Ukr. J. Chem*., **2022**, *10*, 70–83.
27. S. A Umoren, I. B. Obot and E. E. Ebenso, *Eur. J. Chem*., **2008**, *5*, 355–364.
28. A. Al-Amiery, A. S. Taghried, K. F. Alazawi, L. M. Shaker, A. A. Kadhum and M. S. Takriff., *Int. J. Low-Carbon Technol*. **2020**, *15*, 202–208.
29. E. Akbas, S. Celik, E. Ergan and A. Levent., *J. Chem. Sci*., **2019**, *30*, 131–138.
30. K. R. Ansari and M. A. Quraishi., *Phys. E*, **2015**, *69*, 322–329.